Improvement of light quality by ZrO_2 film of chip on glass structure white LED

Huang-Yu Lin,[1] Zhi-Ting Ye,[1] Chien-Chung Lin,[2,3] Kuo-Ju Chen,[1] Hsien-Hao Tu,[1] Huang-Ming Chen,[1] Cheng-Huan Chen,[1] and Hao-Chung Kuo[1,*]

[1]*Department of Photonics & Institute of Electro-Optical Engineering, National Chiao Tung University, Hsinchu 30010, Taiwan*

[2]*Institute of Photonic System, National Chiao Tung University, Tainan 711, Taiwan*

[3]*chienchunglin@faculty.nctu.edu.tw*

[*]*hckuo@faculty.nctu.edu.tw*

Abstract: A novel combination of blue LED chips, transparent glass substrates and phosphors with PDMS thin film is demonstrated. The flip-chip bonding technology is applied to facilitate this design. The ZrO_2 nanoparticles are also doped into the PDMS film to increase light scattering. The resultant luminous efficiency shows an 11% enhancement when compared to the regular COG device. The variation of correlated color temperature of such devices is also reduced to 132K. In addition to these changes, the surface temperature is reduced from 121°C to 104°C due to good thermal dissipation brought by ZrO_2 nanoparticles.

OCIS codes: (230.3670) Light-emitting diodes; (230.2090) Electro-optical devices.

References and links

1. S. Nakamura, T. Mukai, and M. Senoh, "Candela-class high-brightness InGan/AlGan double-heterostructure blue-light-emitting diodes," Appl. Phys. Lett. **64**(13), 1687–1689 (1994).
2. Y. Narukawa, M. Sano, M. Ichikawa, S. Minato, T. Sakamoto, T. Yamada, and T. Mukai, "Improvement of Luminous Efficiency in White Light Emitting Diodes by Reducing a Forward-bias Voltage," Jpn. J. Appl. Phys. **46**(Part 2), 36–40 (2007).
3. M. R. Krames, O. B. Shchekin, R. Mueller-Mach, G. O. Mueller, L. Zhou, G. Harbers, and M. G. Craford, "Status and future of high-power light-emitting diodes for solid-state lighting," J. Disp. Technol **3**(2), 160–175 (2007).
4. A. Chitnis, J. Sun, V. Mandavilli, R. Pachipulusu, S. Wu, M. Gaevski, V. Adivarahan, J. P. Zhang, M. Asif Khan, A. Sarua, and M. Kuball, "Self-heating effects at high pump currents in deep ultraviolet light-emitting diodes at 324 nm," Appl. Phys. Lett. **81**(18), 3491–3493 (2002).
5. Y. C. Yang, J.-K. Sheu, M.-L. Lee, S.-J. Tu, F.-W. Huang, W.-C. Lai, S. Hon, and T. K. Ko, "Vertical InGaN light-emitting diodes with a sapphire-face-up structure," Opt. Express **20**(1), A119–A124 (2012).
6. J. O. Song, D.-S. Leem, J. Kwak, O. Nam, Y. Park, and T.-Y. Seong, "Low resistance and reflective Mg-doped indium oxide-Ag ohmic contacts for flip-chip light-emitting diodes," IEEE Photonics Technol. Lett. **16**(6), 1450–1452 (2004).
7. J. Wierer, D. Steigerwald, M. Krames, J. O'shea, M. Ludowise, G. Christenson, Y.-C. Shen, C. Lowery, P. Martin, S. Subramanya, W. Götz, N. F. Gardner, R. S. Kern, and S. A. Stockman, "High-power AlGaInN flip-chip light-emitting diodes," Appl. Phys. Lett. **78**(22), 3379–3381 (2001).
8. S. J. Chang, C. S. Chang, Y. K. Su, C. T. Lee, W. S. Chen, C. F. Shen, Y. P. Hsu, S. C. Shei, and H. M. Lo, "Nitride-based flip-chip ITO LEDs," IEEE Trans. Adv. Packag. **28**(2), 273–277 (2005).
9. O. B. Shchekin, J. E. Epler, T. A. Trottier, T. Margalith, D. A. Steigerwald, M. O. Holcomb, P. S. Martin, and M. R. Krames, "High performance thin-film flip-chip InGaN–GaN light-emitting diodes," Appl. Phys. Lett. **89**(7), 071109 (2006).
10. M.-Y. Tsai, C.-Y. Tang, C.-Y. Yen, and L.-B. Chang, "Bump and underfill effects on thermal behaviors of flip-chip LED packages: Measurement and modeling," IEEE Trans. Device Mater. Reliab. **14**(1), 161–168 (2014).
11. D. S. Wuu, W. K. Wang, K. S. Wen, S. C. Huang, S. H. Lin, S. Y. Huang, C. F. Lin, and R. H. Horng, "Defect reduction and efficiency improvement of near-ultraviolet emitters via laterally overgrown GaN on a GaN/patterned sapphire template," Appl. Phys. Lett. **89**(16), 161105 (2006).
12. R. Horng, D. Wuu, S. Wei, M.-F. Huang, K. Chang, P. Liu, and K. Lin, "AlGaInP/AuBe/glass light-emitting diodes fabricated by wafer bonding technology," Appl. Phys. Lett. **75**(2), 154–156 (1999).
13. F. Kish, F. Steranka, D. DeFevere, D. Vanderwater, K. Park, C. Kuo, T. Osentowski, M. Peanasky, J. Yu, R. Fletcher, D. A. Steigerwald, M. G. Craford, and V. M. Robbins, "Very high-efficiency semiconductor

#248182 Received 24 Aug 2015; revised 25 Oct 2015; accepted 6 Nov 2015; published 22 Dec 2015

wafer-bonded transparent-substrate (AlxGa1− x) 0.5 In0. 5P/GaP light-emitting diodes," Appl. Phys. Lett. **64**(21), 2839–2841 (1994).
14. C.-L. Chang-Chien, Y.-C. Huang, M.-C. Yip, and W. Fang, "'Flip glass substrate'package technology for LED yield and performance enhancement," J. Micromech. Microeng. **22**(10), 105039 (2012).
15. J. Sun, H. Fatima, A. Koudymov, A. Chitnis, X. Hu, H. Wang, J. Zhang, G. Simin, J. Yang, and M. Asif Khan, "Thermal management of AlGaN-GaN HFETs on sapphire using flip-chip bonding with epoxy underfill," IEEE Electron Device Lett. **24**(6), 375–377 (2003).
16. G. Becker, C. Lee, and Z. Lin, "Thermal conductivity in advanced chips: Emerging generation of thermal greases offers advantages," Adv. Packag. **14**, 14 (2005).
17. N. Caron, M. Bernier, D. Faucher, and R. Vallée, "Understanding the fiber tip thermal runaway present in 3 μm fluoride glass fiber lasers," Opt. Express **20**(20), 22188–22194 (2012).
18. X. Dai, Y. Jiang, C. Hang, Z. Bi, and L. Ma, "Thermal analysis of optical reference cavities for low sensitivity to environmental temperature fluctuations," Opt. Express **23**(4), 5134–5146 (2015).
19. S. Lee, J.-Y. Hong, and J. Jang, "Multifunctional graphene sheets embedded in silicone encapsulant for superior performance of light-emitting diodes," ACS Nano **7**(7), 5784–5790 (2013).
20. Y.-K. Su, P.-C. Wang, C.-L. Lin, G.-S. Huang, and C.-M. Wei, "Enhanced Light Extraction Using Blue LED Package Consisting of TiO_2-Doped Silicone Layer and Silicone Lens," IEEE Electron Device Lett. **35**, 575–577 (2014).
21. H. Misawa, Y. Nishijima, K. Ueno, S. Juodkazis, V. Mizeikis, M. Maeda, and M. Minaki, "Tunable single-mode photonic lasing from zirconia inverse opal photonic crystals," Opt. Express **16**(18), 13676–13684 (2008).
22. X. Fu, A. Melnikaitis, L. Gallais, S. Kiáčas, R. Drazdys, V. Sirutkaitis, and M. Commandré, "Investigation of the distribution of laser damage precursors at 1064 nm, 12 ns on Niobia-Silica and Zirconia-Silica mixtures," Opt. Express **20**(23), 26089–26098 (2012).
23. K.-J. Chen, H.-V. Han, H.-C. Chen, C.-C. Lin, S.-H. Chien, C.-C. Huang, T.-M. Chen, M.-H. Shih, and H.-C. Kuo, "White light emitting diodes with enhanced CCT uniformity and luminous flux using ZrO_2 nanoparticles," Nanoscale **6**(10), 5378–5383 (2014).
24. H.-C. Chen, K.-J. Chen, C.-C. Lin, C.-H. Wang, H.-V. Han, H.-H. Tsai, H.-T. Kuo, S.-H. Chien, M.-H. Shih, and H.-C. Kuo, "Improvement in uniformity of emission by ZrO_2 nano-particles for white LEDs," Nanotechnology **23**(26), 265201 (2012).
25. M. Lallemant, G. Bertrand, J. C. Cannot, J. P. Larpin, N. Roudergues, and M. Assire, "Chemical bistability with thermal feedback effect in the oxidation of titanium-43 wt.-% zirconium alloy," Reactivity of Solids **3**(3), 227–239 (1987).
26. D. Yang, R. Raj, and H. Conrad, "Enhanced Sintering Rate of Zirconia (3Y-TZP) Through the Effect of a Weak dc Electric Field on Grain Growth," J. Am. Ceram. Soc. **93**(10), 2935–2937 (2010).
27. K. Vanmeensel, A. Laptev, H. Sheng, I. Tkachenko, O. Van der Biest, and J. Vleugels, "Experimental study and simulation of plastic deformation of zirconia-based ceramics in a pulsed electric current apparatus," Acta Mater. **61**(7), 2376–2389 (2013).
28. Q. Ashton Acton, *Aluminum Compounds—Advances In Research and Application 2013* (ScholarlyEditions, 2013).
29. F. Incropera, and D. DeWitt, *Introduction to Heat Transfer* (Wiley, 1985).
30. H.-Y. Lin, K.-J. Chen, S.-W. Wang, C.-C. Lin, K.-Y. Wang, J.-R. Li, P.-T. Lee, M.-H. Shih, X. Li, H.-M. Chen, and H. C. Kuo, "Improvement of light quality by DBR structure in white LED," Opt. Express **23**(3), A27–A33 (2015).

1. Introduction

As the energy resources are dwindling these days, it is important to develop the eco-friendly technologies to promote human being's living. The white light-emitting diodes (LEDs) have been one of the green technologies to replace the conventional incandescent light bulbs [1–3]. In the past, the vertical contact types of LEDs were the dominant design. However, the poor thermal conductivity and insulating substrate pose difficulties in application [4]. To deal with this issue, flip-chip technology becomes popular in recent years because it can induce high light-extraction efficiency and good heat dissipation [5–7]. In the flip-chip scheme, an increase of output power can be observed due to the reflector at the bottom and direct bonding of the contact pads which can reduce the shadowing effect [8, 9]. Further investigation of thermal resistance and junction temperature of these flip-chip bonded devices revealed that direct metal contact and less sapphire substrate can really help heat dissipation [10].

In order to generate the high efficiency white LED, there were many approaches to optimize the performance of the w-LED. One of the important techniques is the application of the nanoscale structures that could increase the light extraction. Delicate designs, such as the sapphire substrate with the high aspect ratio cone-shape, and nano-patterned air voids between

#248182 Received 24 Aug 2015; revised 25 Oct 2015; accepted 6 Nov 2015; published 22 Dec 2015

the GaN nano-pillars or the overgrown GaN layer [11], were fabricated on the pattern sapphire substrate to improve the light extraction. In universal, the conventional LED chips were bonded on the opaque substrate to fabricate the SMD (Surface-Mount-Device) type LED package. This type of package can induce certain amount of photon re-absorption such that the degradation of efficiency can be expected. In order to promote the luminous efficiency, the structure of the chip on glass is the good candidate [12, 13]. The highly transparent glass substrate can open up another chance to collect the back-scattered photons and promote the luminous efficiency of the LED. Many results with similar idea have been reported previously. Chien *et al.* designed a flip glass substrate package to enhance the color bin yield, and Chang *et al.* promoted the technology of the flip chip bonding on the ITO [14, 15]. However, to use the glass as the substrate would cause the device operating at higher temperature due to the poor thermal conductivity (σ~1 W/mK), and the low emissivity (the value is about 0.8~0.85) of the glass [16–18]. There were many approaches to resolve this heat dissipation problem such as nanoparticles deployment. In the past, graphene nanoparticles were embedded in the LED package to provide good thermal conduction and extra environment protection [19]. Su *et al.* also investigated the usage of TiO2-doped silicone layer in the LED package [20]. When it was combined with silicone lens, both light extraction and junction temperature can be improved.

This study generated the high luminous efficiency w-LED by the COG (chip on glass) packaging process. One new material, zirconia nanoparticles, could provide a superior photon scattering ability [21–24]. At the same time, the use of the zirconia particles could promote the heat radiation and reduce the temperature of the device due to the high emissivity (the value is 0.95) [25–27]. In this study, ZrO_2 nanoparticles are used with the PDMS film to optimize the performance of the w-LED with the flip chip bonding upon the glass substrate.

2. Experimental methods

This study demonstrates two kinds of host structures by the use of the zirconia particles to yield the white light chip on glass (COG). One is to mix ZrO_2 directly with phosphor/PDMS slurry and the other is to mix the ZrO_2 with silicone to form a diffusing film and then cover this film on the regular phosphor + LED structure. Figure 1(a) shows the schematic and actual structure photograph of the ZrO_2 embedded phosphor PDMS film combining with the COG structure to yield the w-LED. The ZrO_2 particles are blended with the silicone to form the transparent PDMS film and then covered on the COG structure as shown in Fig. 1(b). The YAG phosphor film was dispensed on the COG structure and pumped by the blue chips to generate the white light LED as shown in Fig. 1(c).The fabrication procedure is described as below: First, prepare the LED chips with the wavelength 450nm and flip-chip bond them on the sapphire substrate and covered with the 10wt% YAG phosphor film as the reference sample. Second, mix the zirconia nanoparticles in the silicone slurry and the 10wt% YAG phosphor silicone slurry. Then spin-coat the mixture on the glass and dry it later in order to form the zirconia films. Finally, peel the zirconia/phosphor film from the glass and then put the film on the COG structure with the ZrO_2 of 1wt%, 5wt% and 9wt% to as the Sample1, Sample2, and Sample3, respectively. In the other hand, Sample4, Sample5, and Sample6 are covered by the transparent 1wt%, 5wt% and 9wt% ZrO_2 film on the w-LED device (10wt% phosphor film covered on the COG structure), respectively. Table 1 shows the PDMS films with the different doping concentrations of ZrO_2 particles and phosphors to fabricate the reference sample and Sample1- Sample6.

#248182 Received 24 Aug 2015; revised 25 Oct 2015; accepted 6 Nov 2015; published 22 Dec 2015

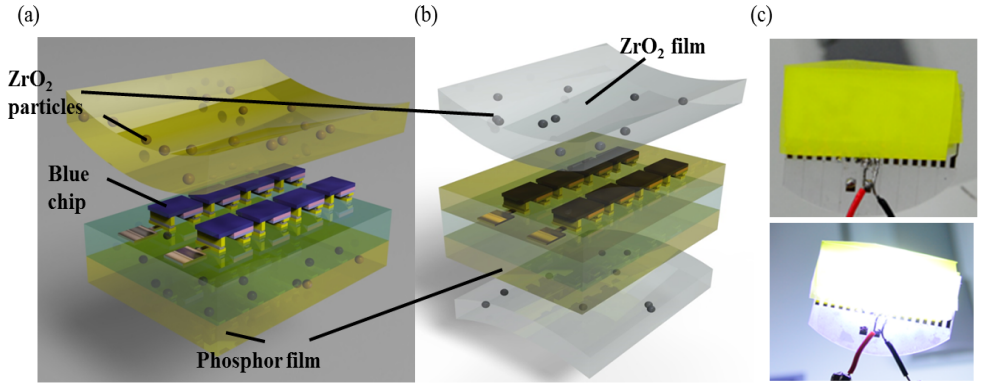

Fig. 1. (a) The cross section of the w-LED combines with the zirconia conjunction phosphor film and COG structure, and (b) the zirconia cover on COG w-LED. (c) The w-LED device combines with the COG structure and the zirconia conjunction phosphor film.

Table 1. The PDMS films are with different weight percent of the ZrO_2 particles and phosphors doping.

	Ref.	Sample1	Sample2	Sample3	Sample4	Sample5	Sample6
ZrO_2 (wt%)	0	1	5	9	1	5	9
Phosphor (wt%)	10	10	10	10	0	0	0

The finished ZrO_2 layer and their mixture with phosphors were inspected by SEM. Figure 2(a) and 2(b) show the SEM cross section images of the ZrO_2 PDMS film and the YAG phosphor/ZrO_2 film. In these images, the thickness of the transparently ZrO_2 PDMS film is about 260.2μm, the YAG phosphor/ZrO_2 film is about 290μm. Figure 2(c) shows that the PDMS film used in this experiment with a particle size is average about 300nm.

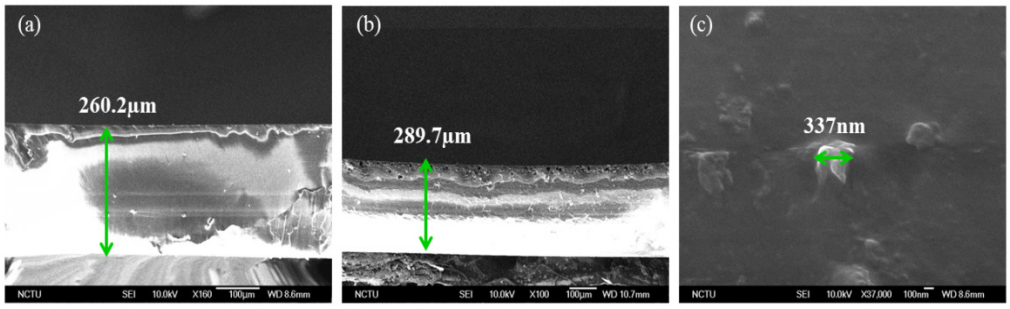

Fig. 2. The cross section view of the (a) ZrO_2 film, (b) the phosphor and ZrO_2 conjunction film, and the (c) ZrO_2 nano-particles in the silicone.

3. Results and discussion

Figure 3(a) shows the spectrum for the reference sample, and other samples with different concentrations of ZrO_2 and phosphors at 80mA of driving current. Furthermore, the CCT and the luminous efficiency are shown in Table 2. In general, the samples with zirconia particles and phosphors perform better than the reference. If only zirconia particles are presented, proper concentration is needed to enhance the luminous efficiency. The phenomena are caused by the high scatting ability of the ZrO_2 nanoparticles and the improvement results from the better utilization of the blue photons from the LEDs [24]. In order to receive highest lumen efficiency, the best ratio of the ZrO_2 blended phosphor film and the pure ZrO_2 layer is about 1wt% and 5wt%, respectively. However, as the ratio of the zirconia nanoparticles increasing above 5wt%, it can cause lower luminous efficiency because high concentration of

#248182 Received 24 Aug 2015; revised 25 Oct 2015; accepted 6 Nov 2015; published 22 Dec 2015

the ZrO_2 would led the extra light trapping and re-absorption of the emitted photons and reduce the transmittance of the layer [24, 25]. Figure 3(b) shows the COG structure w-LED sample with and without ZrO_2 layer after 10 minute driving at 80mA. The lumen efficiency of all the COG w-LED samples would decay after driving the devices after 10 minutes. The phenomenon is caused by the poor thermal conductivity and the low emissivity. Due to this low thermal conductivity of the glass substrate, after 10 minutes of electrical driving, the heat dissipation is poor and the package temperature rises accordingly. The lumen efficiency and the CCT of the reference sample and Sample1 to Sample6 after the 10 minutes driving are listed in Table 3. As shown in Table 3, the 5wt% ZrO_2 blended phosphor layer with the excellent performance after the time passes. In addition to the spectral intensity change, the efficiency (lumen/watt) of the w-LEDs can be modified after 10 minutes of 80mA continuous arriving. From Fig. 3(c), all samples show some degradation on efficiency, but the reference ones (without any ZrO_2) degrade most, and the amount of degradation drops as the weight percent of ZrO_2 increases. We believe the high emissivity of ZrO_2 particles (0.95) plays an important role on this phenomenon because they can effectively reduce the internal temperature of the package.

Table 2. The luminous efficiency and CCT for the reference and zirconia layer combined sample

	Ref.	Sample1	Sample2	Sample3	Sample4	Sample5	Sample6
CCT(K)	4960.1	4736.6	4912	4737	4883	4911.3	4956
Lumen/watt	176.7	196.8	194.4	189.8	188.9	196.1	174.1

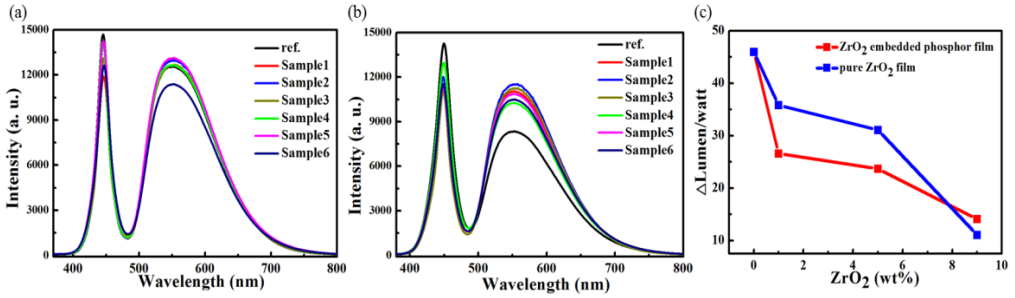

Fig. 3. (a) The emission spectra for the reference sample, ZrO_2 embedded phosphor film covered samples and the reference sample covered by the ZrO_2 film at 80mA and (b) the emission spectra after 10 minutes driving. (c) The deviation of the lumen efficiency between the original samples and after 10minutes driving samples.

Table 3. The luminous efficiency and CCT for the reference and zirconia layer combined sample after 10 minutes driving

	Ref.	Sample1	Sample2	Sample3	Sample4	Sample5	Sample6
CCT(K)	6364.5	5010.1	4859	4807.7	5421.8	5042	6275.1
Lumen/watt	130.4	170.2	181.8	178.3	153.1	165	163

To verify this conjecture, we need to check the actual temperature of these units. Figure 4(a)-4(d) shows the w-LED with ZrO_2 nanoparticles in operation the surface temperature mapping illustrations. According to the thermal images, the white area represents the maximum surface temperature plotted in the Fig. 4(e) and 4(f). The surface temperatures shown in the figures were measured after 10 minutes of continuous electrical injection with different configurations, the devices demonstrated various temperatures. The temperature differences between the two groups (Sample 1-3 vs Sample 4-6) rise from the different layout in the COG package. In Sample 1-3, there are two phosphor films with ZrO_2 embedded. However, for Sample 4-6, there is one additional ZrO_2/silicone layer because the phosphor and ZrO_2 layers are separated. This additional layer can increase the total temperature by 5°C

#248182 Received 24 Aug 2015; revised 25 Oct 2015; accepted 6 Nov 2015; published 22 Dec 2015

due to poorer heat dissipation in the device. As these results showed, the combination of the ZrO_2 nanoparticles embedded layer can reduce the surface temperature of the w-LED and resolve the poor heat dissipation of the sapphire for the COG structure effectively.

To understand the possible explanation on the measured surface temperature results, the correlation between the packaged material and heat transfer needs to be clarified. It is true that the higher concentration of ZrO2 can lead to more photon trapping and thus potentially more re-absorption and more temperature rising. In a general LED scheme, about 20% of input power turns into optical energy and 80% becomes heat [28]. These 20% of photons will have about 30% of them becomes stray photons and possibly get re-absorbed in the package. So if we just consider the source of this trapped or re-absorbed photons in terms of total input power, 6% at most of extra heat (20% × 30%) can be generated due to this re-absorption. Comparing to the original heat directly from LED chip, this is a far smaller portion. On the other hand, the high emissivity of the ZrO_2 nanoparticles helps the film to relieve from this extra heat generation. From the general theory of heat transport provided in the previous question, the radiation and convection parts are significant when the film to the environment temperature difference is high. Although the number of trapped photons is high, the presence of ZrO_2 can radiate more heat out and thus lower the overall temperature of the package.

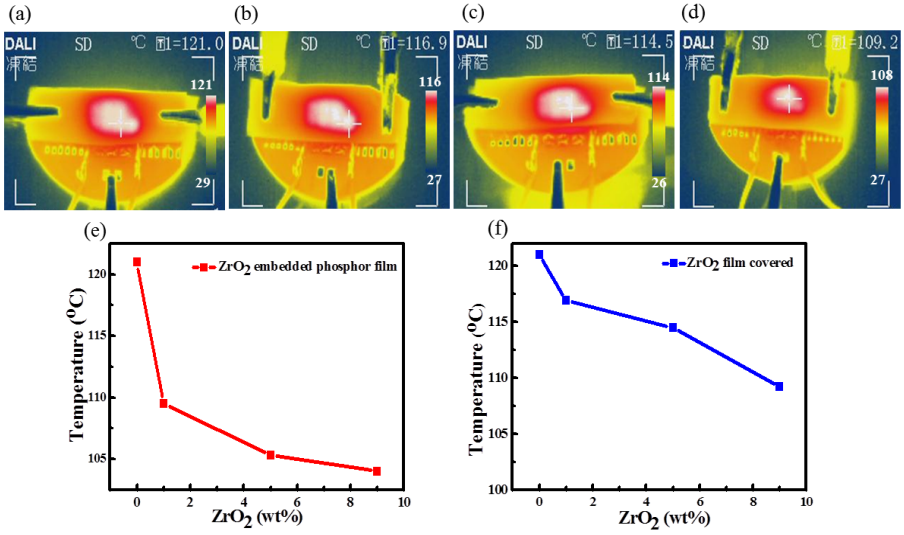

Fig. 4. (a)-(d) The surface temperature mapping of the COG structure w-LED combine with the zirconia after the 10 minute driving. The surface temperature diversification of (e) the ZrO_2 nanoparticles with different ratio doping in the phosphor film w-LED samples and (f) the ZrO_2 layer covered on the top of the w-LED samples after the 10 minute driving.

Figure 5 shows the CIE 1931 coordinates of the initial and after 10 minutes of continuous driving. The effect of this 10-minute driving in the reference samples can be observed clearly as the CIE coordinates change before and after, which is not desirable for solid state lighting. On the other hand, all other samples show very little change in the CIE 1931 coordinates, which is a good sign and also can be viewed as another indicator of improvement brought by ZrO_2.

#248182 Received 24 Aug 2015; revised 25 Oct 2015; accepted 6 Nov 2015; published 22 Dec 2015

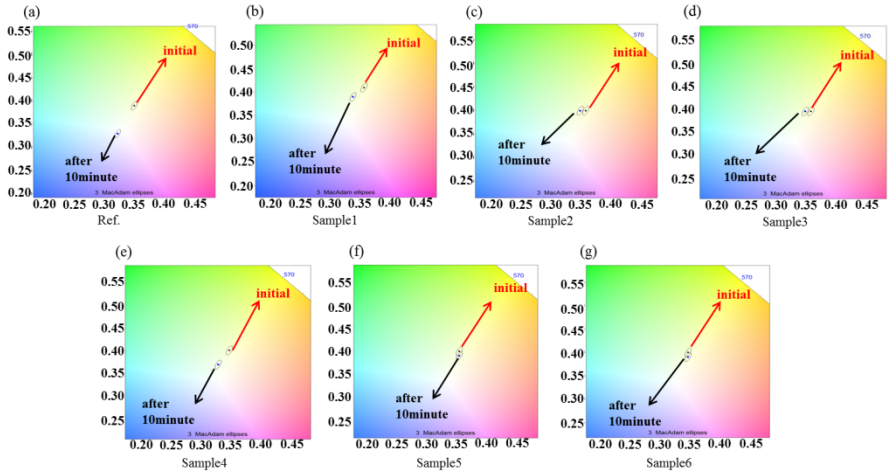

Fig. 5. The variation of the CIE1931 coordinates between the original samples and after 10minutes driving samples

Table 4 shows that the thermal conductivity of the phosphor films changed with the application of ZrO_2 nanoparticles. In this table, the thermal conductivity increases as the concentration of the ZrO_2 increases.

Table 4. The thermal conductivity of the PDMS film with the different concentrates

ZrO_2 concentration	0wt%	1wt%	5wt%	9wt%
Thermal conductivity(W/ m^2K)	0.528	0.735	0.739	0.821

To consider the full thermal effect in the mixed film, we must include different components in heat transport: the radiation, convection and conduction terms. The effect caused by the thermal conductivity of the phosphor films is very weak in the total heat transfer rate of the LED. The thermal properties between the phosphor/ZrO_2 films and the w-LED can be described by the Eqs. (1)-(4) are calculated using as below [29]:

$$Q_{cond} = kA\left(T_s - T_a\right)d^{-1} \tag{1}$$

$$Q_{rad} = \varepsilon\sigma A\left[\left(T_s\right)^4 - \left(T_a\right)^4\right] \tag{2}$$

$$Q_{conv} = HA\left(T_s - T_a\right), H = \varepsilon\sigma A\left(T_s + T_a\right)\left[\left(T_s\right)^4 + \left(T_a\right)^4\right] \tag{3}$$

$$\begin{aligned} Q_{total} &= Q_{conv} + Q_{rad} + Q_{cond} \\ &= \varepsilon\sigma A\left(T_s + T_a\right)\left[\left(T_s\right)^4 + \left(T_a\right)^4\right] + \varepsilon\sigma A\left[\left(T_s\right)^4 - \left(T_a\right)^4\right] + kA\left(T_s - T_a\right)d^{-1} \end{aligned} \tag{4}$$

In these formulas, Q_{cond}, Q_{rad} and Q_{conv} are defined as the thermal conduction, radiation and convection heat transfer rate for the exterior surface of w-LED, respectively. The total heat transfer rate formula of the w-LEDs is calculated as shown in Eq. (4). Where k is the thermal conductivity, A is the surface area, d is the thickness, ε is the emissivity, σ is Stefan-Boltzmann constant, H is the convection heat transfer coefficient, T_s and T_a is the surface temperature and surround temperature of the device, respectively. By the formula, the main effect for the total heat transfer rate is the combination of the Q_{conv} and Q_{rad} because the influencing factor of the sum for the value: $\varepsilon\sigma A\ (T_s + T_a)\ [(T_s)^4 + (T_a)^4]$ and $\varepsilon\sigma A\ [(T_s)^4 - (T_a)^4]$ is much larger than the factor of conduction heat transfer rate: $kA\ (T_s - T_a)d^{-1}$. As the result, the radiation and convection terms are dominant in heat transfer and the emissivity (ε) is more

#248182 Received 24 Aug 2015; revised 25 Oct 2015; accepted 6 Nov 2015; published 22 Dec 2015

important than the thermal conductivity. Figure 1 shows the simulation results of the COG structure covered with the different emissivity materials and refers from the Eqs. (1)-(4) by the Flow simulation software. All the factors of the total thermal properties have been considered, such as the surface area, thermal conductivity, and emissivity.

To verify the assumption of emissivity of ZrO_2 on the package temperature, we set up a numerical environment to simulate the outcome. Figure 6 shows the simulation results of the COG structure covered with the different emissivity materials refers from the Eqs. (1)-(4) by the Flow simulation software. The simulation is executed based on the structure in Fig. 6(a), covered with the thin film mixing with the different concentration (0wt%, 49wt%, 99wt%) of ZrO_2 particles to produce the silicone thin films with the different emissivity(0.7, 0.85, 0.95), respectively. Figure 6(b)-6(d) shows the thermal image of the COG structure covered by the thin film and the temperature of the chip is about 96.7°C (emissivity 0.7), 94.4°C(emissivity 0.85), and 92.8°C(emissivity 0.9), respectively. From our calculation, the surface temperature reduces significantly when the emissivity of the composite film increases and other parameters are kept the same.

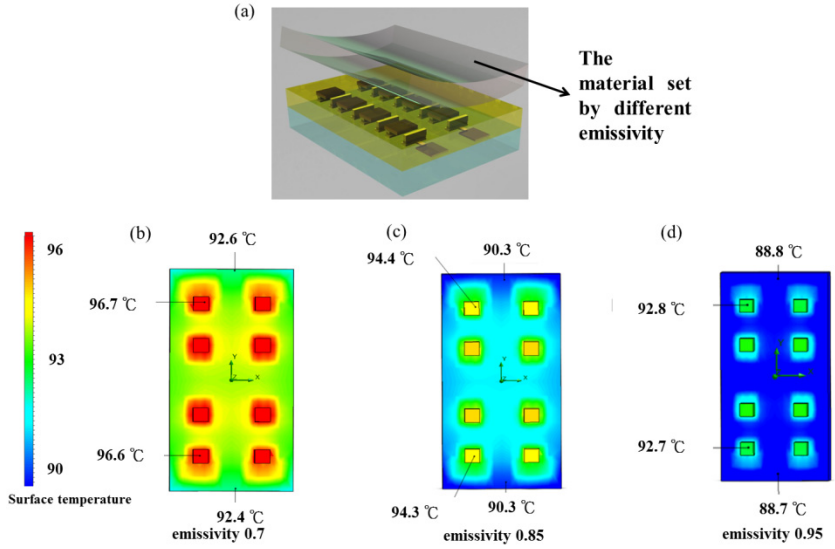

Fig. 6. The modulation emissivity simulation result of the COG structure w-LEDs.

The color uniformity of the w-LED can be evaluated by the deviation of correlated color temperature (ΔCCT) which is defined as the difference between the CCT(max) and the CCT(min) [24] Beside the nice heat dissipation ability, the ZrO_2 nanoparticles are also known for the excellent scattering capability which can improve the uniformity of the CCT [30]. As shown in Fig. 7, the diagram shows the Sample1 to Sample6 with angular distribution of CCT at the current of 80 mA. The CCT deviations for the reference sample, the phosphor and ZrO_2 nanoparticles blended PDMS COG w-LEDs (Sample1 to Sample3) is about 420K, 336K and 162K, and the other w-LED samples with the additional the transparent ZrO_2 PDMS layer (Sample4 to Sample6) is about 833K, 721K and 434K, respectively. As these results, the use of ZrO_2 nanoparticles embedded PDMS film can improve the color uniformity of the w-LED, and the phosphor films doped by ZrO_2 nanoparticles are perform better than the samples with the additional transparent ZrO_2 PDMS layer. The reason is that the zirconia particles in the phosphor film have a smoother angular-dependent CCT distribution than the ZrO_2 nanoparticles embedded in the PDMS film on the surface of the phosphor layer, because which can provide an effective scattering to the excite the around phosphor particles. The haze intensity image permit the doped phosphor films are with the excellent diffuse ability than the covered of the additional transparent ZrO_2 PDMS layers on the phosphor films as

#248182 Received 24 Aug 2015; revised 25 Oct 2015; accepted 6 Nov 2015; published 22 Dec 2015

shown in Fig. 7(b) However, that would influence the CCT deviations when the concentrate of the ZrO_2 nanoparticles increase more than 9%, the best ratio is about 5%.

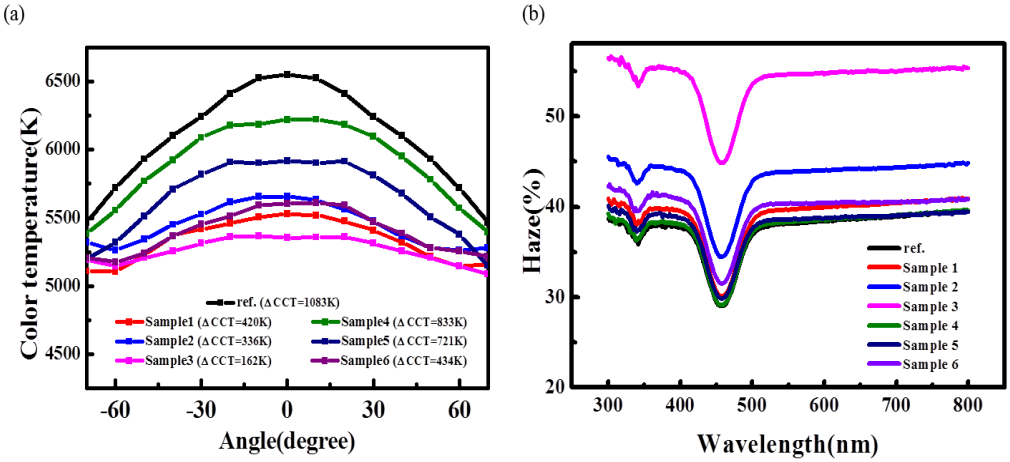

Fig. 7. (a) The spectrum of angular-dependent CCT at 80mA and (b) the haze intensity of the reference sample and Sample1 to Sample6.

4. Conclusion

This study demonstrates a highly efficient design of w-LED with COG structure and ZrO_2 PDMS films. The w-LED can obtain the least CCT deviations (132K) in the case of the 5wt% ZrO_2 blended phosphor film and the use of the ZrO_2 film can improve the color uniformity of the w-LED effectively. The phosphor film blended of the 1wt% zirconia particles can improve the luminous efficiency of the w-LED and achieve a 11% enhancement than the COG w-LED without the ZrO_2 film covered. The ZrO_2 blended phosphor film and pure ZrO_2 film can reduce the surface temperature of the COG w-LEDs from 120°C to the 110°C and the ZrO_2 blended phosphor film is more effective than the pure ZrO_2 film in terms of thermal dissipation. The high emissivity of ZrO_2 can help on this heat dissipation and this is verified via simulation and experiments. In conclusion, it is very useful to resolve the heat dissipation problem and improve the lumen efficiency by the combination of the ZrO_2 PDMS films with the COG structure w-LEDs.

Acknowledgment

The authors express their gratitude to Epistar for their technical support. This research was funded by the National Science Council, Taiwan (NSC102-3113-P-009-007-CC2, NSC 103-3113-E-009-001-CC2, and NSC 103-2917-I-009-179).

#248182 Received 24 Aug 2015; revised 25 Oct 2015; accepted 6 Nov 2015; published 22 Dec 2015